https://doi.org/10.5194/egusphere-2024-922
Preprint. Discussion started: 29 April 2024

Historically consistent mass loss projections of the Greenland ice sheet.

Charlotte Rahlves[1,2], Heiko Goelzer[1], Andreas Born[2], and Petra M. Langebroek[1]

[1]NORCE, Norwegian Research Centre, Bjerknes Centre for Climate Research, Bergen, Norway
[2]Department of Earth Science, University of Bergen, Bjerknes Centre for Climate Research, Bergen, Norway

Correspondence: Charlotte Rahlves (chra@norceresearch.no)

Abstract. Mass loss from the Greenland ice sheet is presently a significant factor for global sea-level rise and is expected to increase under continued Arctic warming. As sea-level rise is threatening coastal communities worldwide, reducing uncertainties in projections of future sea-level contribution from the Greenland ice sheet is of high importance. In this study we determine sea-level contribution that can be expected from the ice sheet until 2100 by performing an ensemble of stand-alone ice sheet simulations with the Community Ice Sheet Model (CISM). The ice sheet is initialized to resemble the presently observed geometry by calibrating basal friction parameters. We use forcing from various Earth System Models (ESMs), as well as from ERA5 reanalysis for initialization and investigate how this affects the simulated historical mass loss and the projected sea-level contribution until 2100. The observed historical mass loss is generally well reproduced by the ensemble, with a particularly close match with observations when using output from ERA5 reanalysis to force the initialization as well as the historical run. We examine a range of uncertainties, associated with stand-alone ice sheet modeling by prescribing forcing from various ESMs for three different emission scenarios. Atmospheric forcing is downscaled with the regional climate model MAR. Retreat of marine-terminating outlet-glaciers in response to ocean forcing and runoff from the ice sheet is represented by a retreat parameterization and its uncertainty is sampled by considering different sensitivities. Furthermore, we disentangle the relative importance of surface mass balance (SMB) and outlet-glacier retreat forcing, as well as of the SMB-height feedback, on the projected mass loss by performing dedicated single forcing experiments. While discharge from outlet-glaciers remains a substantial factor, the future evolution of the ice sheet is governed by mass loss due to changes in SMB. Assuming a medium sensitivity to outlet-glacier retreat forcing, by 2100, the projections yield a sea-level contribution of 32 to 69 mm under the SSP1-2.6 scenario, 44 to 119 mm under the SSP2-4.5 scenario and 74 to 228 mm under the SSP5-8.5 scenario. With a spread of 154 mm under the SSP5-8.5 scenario climate forcing constitutes the largest source of uncertainty for the projected sea-level contribution, while uncertainty in the retreat forcing account for a spread of 25 mm. We find differences in projected sea-level contribution due to the initial state of the ice sheet and grid resolution to be minor.

1 Introduction

Increased mass loss from the Greenland ice sheet is expected to be a major contributer to future global sea-level rise. The two main mechanisms causing this mass loss are decreasing SMB and increasing ice discharge via outlet glaciers interacting with

https://doi.org/10.5194/egusphere-2024-922
Preprint. Discussion started: 29 April 2024

ocean water. Estimates of the relative importance of both processes indicate that, in recent decades, SMB has been responsible for about 50 to 75 % of Greenland's mass loss, while discharge from marine terminating glaciers accounts for the remainder (Enderlin et al., 2014; Shepherd et al., 2012; Broeke et al., 2009). Several studies suggest that SMB will increase in importance (Goelzer et al., 2013; Fürst et al., 2015), while outlet glacier dynamics will continue to substantially contribute to the ice sheet's mass loss. On the other hand, recent findings by Choi et al. (2021) suggest that outlet glacier retreat may become an even more prominent factor, potentially contributing up to 56 % of the mass loss by the end of the century under a high emission scenario.

Accurately projecting Greenland's response to future climate is challenging due to various reasons, including uncertainties arising from poorly constrained boundary conditions, model formulations and the inability to adequately resolve or represent all relevant physical processes. With the goal of improving projections of sea-level contribution from ice sheets, several studies have investigated various aspects that contribute to these uncertainties. Goelzer et al. (2013), for example, have evaluated the effects of physical model formulations, such as handling of SMB forcing, outlet-glacier dynamics and basal lubrication, as well as model resolution on projected contributions of the Greenland ice sheet to global sea-level rise. Spatial representation in terms of grid spacing and resolution of bedrock topography, as well as the interaction with outlet glacier forcing were also focus of a study by Rückamp et al. (2020), while the effect of elevation feedback parameterization on modeling results was invested by Edwards et al. (2014). Sea-level projections have been found to be highly sensitive to climate forcing and ice sheet model uncertainty (Bindschadler et al., 2013; Goelzer et al., 2020b). The Ice Sheet Model Intercomparison Project for CMIP6 (ISMIP6), for example, assessed uncertainties related to climate forcing and quantified ice sheet model uncertainty, by comparing projections with different ice sheet models using various climate forcing from the CMIP5 archive (Goelzer et al., 2020b). In accordance with previous studies, ISMIP6 identified the initial representation of the modeled ice sheet as a major source of uncertainty for ice sheet projections. Many simulations showed a large models drift, resulting from the initialization to present day, and insufficient representation of historical mass loss.

The initialization of ice sheet models to represent present-day conditions is a critical aspect of projecting future ice sheet behavior. Past studies have compared various initialization methods and investigated their impacts on projections (Aschwanden et al., 2013; Yan et al., 2013; Adalgeirsdóttir et al., 2014; Goelzer et al., 2018). Initialization of ice sheet models can be done using various approaches, each with distinct advantages and limitations. One possible method involves simulating full glacial cycles that have preceded the present day climate while allowing for the ice sheet geometry to freely evolve, ensuring consistency in surface mass balance (SMB), ice thickness, velocity field, and ice temperature (e.g. Huybrechts and Wolde, 1999; Yang et al., 2022). This approach produces a self-consistent ice sheet that is in balance with its past forcing and provides the ice sheet state with a long-term memory of past conditions. However, so-called paleo spin-ups often result in substantial deviations from observed ice sheet geometries, potentially introducing biases in future projections. As an alternative, data assimilation techniques prioritize matching present-day observations, yielding ice sheet configurations that closely resemble reality (Seroussi et al., 2011; Larour et al., 2012; Gillet-Chaulet et al., 2012; Pollard and Deconto, 2012; Brinkerhoff and Johnson, 2013; Lee et al., 2015). Matching the observed state of the ice sheet is possible using inverse methods or calibration, where poorly constrained parameters are adjusted to achieve a close match with observed surface velocities (e.g. Morlighem et al., 2010; Seroussi et al., 2013; Gillet-Chaulet et al., 2016) or ice sheet surface elevation (e.g. Pollard and Deconto, 2012).

https://doi.org/10.5194/egusphere-2024-922
Preprint. Discussion started: 29 April 2024

However, this method may induce unwanted model drift due to mismatching boundary conditions, model physics or assimilation targets and lack of past climate memory. Inverting for less constrained variables such as bed friction and may thus lead to compensation effects (Berends et al., 2023). Furthermore, issues arise regarding the choice of SMB representation during initialization, as different choices of reference SMB may lead to divergent projections of future mass loss. Several past studies (Pattyn et al., 2013; Seroussi et al., 2014; Goelzer et al., 2018) have emphasized the need to further improve on initialization methods for ice sheet modeling and advocated to further explore combined approaches, which, for example, allow for a relaxation after data assimilation.

Projections of future ice sheet mass loss are often performed using climate forcing in terms of SMB anomalies with respect to a reference SMB (Edwards et al., 2014; Goelzer et al., 2020b; Payne et al., 2021). Forcing with absolute SMB output from a climate model is generally difficult due to the bias that many climate models exhibit (Knutti and Sedláček, 2013; Vial et al., 2013; Eyring et al., 2016). The anomaly approach ensures the removal of biases and allows the combination of SMB forcing from different sources. This is often necessary when simulating a time span that includes the historical period as well as a future projection, or when performing an ensemble of projections that start from the same initial state but use future forcing from various climate models.

In the present study we address the question of initialization by investigating how the use of different initial SMB products for an inverse initialization of the ice sheet impacts the projected mass loss. Additionally, we evaluate the impact of forcing projections with absolute SMB values versus prescribing SMB anomalies, thereby complementing existing estimates of sea-level contribution from the Greenland ice sheet on a decadal to centennial timescale. We sample uncertainties related to climate forcing and modeling choices. Moreover, we perform a suite of single forcing experiments to separate the respective contribution of SMB and outlet-glacier retreat, alongside the SMB-height feedback, in driving the projected mass loss.

In the following section (Sect. 2) we describe the ice sheet model and the experimental set-up, before we present the results in Sect.3. We examine the initial state in Sect. 3.1, the historical period in Sect. 3.2 and the projections in Sect. 3.3. In Sect.3.3.1 we investigate the relative importance of different forcing mechanisms and finally close with a discusses the results in the context of previous studies.

2 Model description and experimental set-up

2.1 The Community Ice Sheet Model

We project contributions to global mean sea-level from the Greenland ice sheet until the year 2100 by performing an ensemble of standalone simulations with the Community Ice Sheet Model (CISM) (Lipscomb et al., 2019), which is a 3-D thermomechanically coupled higher order model. Given the 2D surface elevation and thickness fields, the 3D temperature field, and relevant boundary conditions, the model calculates the ice velocity by solving a depth-integrated-viscosity approximation of the Stokes equations (Goldberg, 2011) on a structured rectangular grid. Simulations in this study are run using 11 vertical layers and a horizontal grid resolution of 4 km, 8 km and 16 km. We apply a power law to describe basal sliding. At the start of the simulation the ice sheet is set to present day conditions using observed bedrock topography and ice surface elevation

https://doi.org/10.5194/egusphere-2024-922
Preprint. Discussion started: 29 April 2024

(Morlighem et al., 2017). The topography data is first smoothed with a Gaussian filter, before it is interpolated onto the model grid using a nearest-neighbor approach. The ice temperature is prescribed with an advective-diffusive balance between the surface temperature at the upper boundary and the geothermal heat flux according to data from Shapiro and Ritzwoller (2004) at the lower boundary. The thermal evolution of the ice sheet is determined by a prognostic temperature solution. Climate forcing at the upper boundary is applied via providing SMB and surface temperature (ST) fields. All floating ice is assumed to calve immediately.

2.2 Climate forcing

Climate forcing for the simulations comes from ten different Earth System Models (ESMs) (nine CMIP6 models and one CMIP5 model), as well as from ERA5 reanalysis (Hersbach et al., 2020). All simulations have been dynamically downscaled over Greenland with the Model Atmospheric Regional (MAR) in version v3.12 (Fettweis et al., 2017). Atmospheric forcing is represented by prescribing either absolute SMB and ST or anomalies. The SMB-elevation feedback, which arises due to a changing ice sheet geometry, is parameterized based on local vertical gradients of runoff. We use this variable rather than gradients in SMB, because it is not affected by precipitation, which does not have a consistent gradient with elevation. Retreat of marine-terminating outlet glaciers is prescribed as maximum ice front position applying a semi-empirical parameterization (Slater et al., 2019, 2020) which uses mean summer runoff from the ice sheet provided by MAR and depth averaged (200 m – 500 m) far-field ocean temperature change from the ESMs aggregated over seven drainage basins around Greenland. Uncertainty in the sensitivity of the outlet glacier retreat to its forcing is sampled using three different values for the sensitivity parameter, which controls the amount of frontal retreat for a given change in ocean temperature and ice sheet runoff. We use medium, low and high sensitivities covering the median, 25 % percentile and 75 % percentile of values from a distribution of calibrated values using observations of retreat for nearly 200 tidewater glaciers over the period of 1960-2018. We use forcing for the low emission scenario SSP1-2.6, the intermediate emission scenario SSP2-4.5 and the high emission scenario SSP5-8.5 to sample a wide range of possible socioeconomic pathways. Furthermore, we examine the relative importance of SMB forcing vs outlet-glacier retreat forcing by performing additional projections where only part of the forcing is activated at a time.

2.3 Experimental set-up

The setup of the simulations is similar to the ISMIP6 protocol (Goelzer et al., 2020b), except for a dedicated historical experiment. Simulations consist of three parts; the spin-up which results in an initial ice sheet assigned to 1960, a historical run from 1960 to 2014 and a projection from 2015 to 2100.

2.3.1 Spin-up

The goal of the spin-up is to to produce an ice sheet that is in balance with its forcing and closely resembles present day conditions. During a period of 5000 years we apply an annual mean SMB and ST of a reference period, which we choose

https://doi.org/10.5194/egusphere-2024-922
Preprint. Discussion started: 29 April 2024

to be 1960-1989, a period during which the ice sheet is assumed to have been in relative balance with its forcing (Broeke et al., 2009). During spin up the basal friction parameters are calibrated to nudge the ice surface elevation towards present-day observations following Pollard and Deconto (2012). The obtained basal friction parameters are then held constant for the rest of the simulation, which we assume to be justified for a centennial timescale. It should be noted that this approach leads to the compensation of other modeling inaccuracies or inaccuracies in forcing through the bed roughness (Berends et al., 2023). To minimize residual model drift, we let all initialized ice sheets relax for an additional 1000 years, for the 4 km grid resolution, and for 500 years for the coarser resolutions on their respective bed friction field before assigning the resulting ice sheet geometry to that of 1960.

We divide our ensemble of projection into two subsets, depending on the use of SMB during spin-up:

1. For the first ensemble we produce one single initialization by applying SMB from ERA5 reanalysis downscaled with MAR, which matches well with observations over the reference period. We call the ensemble using this initialization the ERA5-init ensemble.

2. For the second ensemble we perform multiple spin-ups using the reference SMB from each ESM downscaled with MAR. We thereby obtain multiple initial ice sheets, each with a different friction field and small variations in ice surface elevation. The ensemble using this initialization approach will henceforth be called ESM-init ensemble.

Performing multiple spin-ups is more expensive in terms of computer resources. In addition, most ESMs do not well reproduce the observed mean SMB over the reference period, even when downscaled, as they are often biased, which might lead to a lower quality initialization.

2.3.2 Historical period

We define the historical period to extend from 1960 to 2014.

All runs in the ERA5-init ensemble branch off from the one single ERA5-initialization, which also implies that the friction field is the same for all members of this ensemble. The historical run is forced with SMB and ST from ERA5 reanalysis, which well reproduces observations. Observations of ocean temperature used for the retreat parameterization comes from the Hadley Centre EN4.2.1 dataset (Good et al., 2013) We perform three different historical runs, each using a different sensitivity to the outlet glacier retreat forcing.

The historical runs in ensemble ESM-init branch off each ESM-initialization and are forced with absolute values of SMB and ST from the respective ESM output. Note that ESMs generally do not reproduce the observed interannual and interdecadal variability in SMB over the historical period. Again, each historical run is performed three times using different sensitivities to the outlet-glacier retreat forcing, which is produced using ocean temperature from each ESM .

https://doi.org/10.5194/egusphere-2024-922
Preprint. Discussion started: 29 April 2024

2.3.3 Future projections

Following the historical run, future projection start at 2015 and go out to the year 2100. In both ensembles all three sensitivities to outlet glacier retreat forcing are taken into account.

In the ERA5-init ensemble projections are forced by anomalies with respect to the annual mean SMB and ST of the reference period (1960-1989) from the same ESM that is used for the projection. This approach commonly used approach (e.g. Goelzer et al., 2020b) ensures the use of high quality forcing during spin up and allows for a correction of biases in the ESM forcing. Furthermore, it has the advantage of being computationally efficient, as only one initialization is needed for the entire ensemble of projections. It comes, however, at the cost of introducing a possible inconsistency in the forcing, when transitioning from the ERA5 forced historical simulation to the projection.

For the ESM-init ensemble, projections are forced by prescribing absolute values of SMB and ST, following the approach used for the historical period. Note that values of absolute SMB and surface temperature in ensemble ESM-init can technically be divided into a reference part (annual mean of the ESM over the period of 1960-1989) and an anomaly part. This means that forcing, in terms of anomalies, is identical in both ensembles, because, in both cases, the anomalies are calculated with respect to the ESM annual mean of the reference period. Forcing with absolute SMB from the same source ensures a consistent forcing stream of the simulation from initialization throughout the historical period and the projections.

Bedrock elevation is kept constant throughout the simulation, as we assume isostatic adjustment to be small on a centennial timescale and therefore negligible for the projections (Sutterley et al., 2014; Wake et al., 2016). Sea-level contributions are calculated relative to the year 2015 based on ice volume above flotation and include a density correction that accounts for density differences between ocean water and fresh meltwater (Goelzer et al., 2020a). For conversion of ice volume change to sea-level equivalent we assume a constant ocean area of 3.625×10^{14} (Gregory et al., 2019).

In total we run 304 projections in four forcing modes (of which 192 using full forcing) with forcing from 10 different ESMs, sampling three SSPs, three sensitivities to outlet-glacier retreat forcing, three grid sizes and two different initialization approaches.

3 Results

3.1 Initial state

By the end of the initialization, ice thickness, temperature and velocity fields of all modeled ice sheets are close to steady-state. With a mass change range of -41 Gt to -55 Gt over 100 years, the residual drift is very limited for all models, except for the ACCESS1.3-initialization, which exhibits a drift of -110 Gt over 100 years.

Simulated ice mass ranges from 2.71×10^6 Gt to 2.74×10^6 Gt at the end of the initialization. In comparison, observations of the Greenland ice sheet suggest an ice mass of $2.73 \pm 0.02 \times 10^6$ Gt (assuming the same ice density of 917.0 $\mathrm{kg\,m^{-3}}$ as used for the simulations, instead of an ice density of 916.7 $\mathrm{kg\,m^{-3}}$) (Shepherd et al., 2020). Therefore, the simulations closely align with observational data. The slight variations in the experiment's initial mass can be attributed to the limited ability of

https://doi.org/10.5194/egusphere-2024-922
Preprint. Discussion started: 29 April 2024

the initialization method to compensate for biases in the initial SMB.

Figure 1 shows the ice sheet state after the initialization using forcing from ERA5-reanalysis. The comparison of this initialization to all members of the ESM-init ensemble (see Fig. S1-S3 in the supplements) shows no common pattern. In the following we focus our analysis on the comparison of the ERA5-initialization to the initialization produced with SMB from NorESM2-MM (which is our in house model) in Fig. 2. Differences in SMB are most pronounced around the margins of the ice sheet, where NorESM2-MM generally exhibits higher SMB values than ERA5. This leads to differences in the resulting bed friction fields, which compensate for the difference in SMB during inversion for the same target geometry by increasing the slipperiness in areas where high SMB values produce too thick ice and vice versa. This way, ice is being evacuated more effectively from areas with a surplus, while it is retained in areas where modeled ice thickness is lower than targeted. The inferred bed roughness of the NorESM2-MM initialization is lower, especially in areas of higher SMB, except for parts of the North-West and center region of the ice sheet. While the target geometry is the same for both initializations, the ice sheet thicknesses at the end of the initialization procedure still differ slightly around parts of the margins. This is a residual due to the inability of the inversion process to fully compensate for discrepancies between forcing and target geometry, which, in this case, leads to thicker margins of the initial ice sheet for the NorESM2-MM initialization.

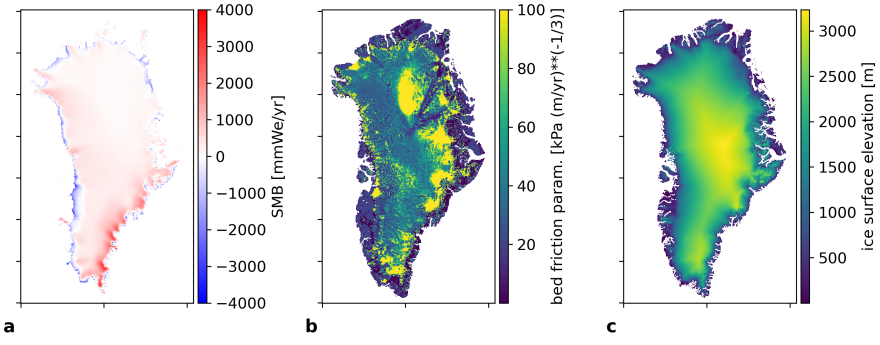

Figure 1. Initial fields of SMB (a), bed friction parameter (b) and ice surface elevation (c) of the ERA5-initialization after a 5000 year spin up and additional 1000 years of relaxation time.

To further explore the calibration process and to examine the ice sheet's response to changes in SMB and friction field during the spin-up we perform two supplementary spin-up runs. We use the ESM-SMB spin-up as a starting point, but exchange the bed friction field with that of the ERA5-initialization and let the ice sheet relax on this friction field for another 1000 years (Fig. 3a). For the second simulation we take the ERA5 spin-up and change the SMB forcing to that of the ESM after the end of the spin-up period (Fig. 3b). Again we let the ice sheet relax in this configuration for another 1000 years. In other words, in the first case the initial ice sheet is spun up using the ESM-SMB, while in the second case the ice sheet is spun up using the ERA-SMB. In both cases the spun up ice sheet is then relaxed on a friction field that originates from the ERA-spin up, while applying the ESM-SMB. The resulting ice sheet geometries deviate from the ERA5-initialization, while closely resembling

https://doi.org/10.5194/egusphere-2024-922
Preprint. Discussion started: 29 April 2024

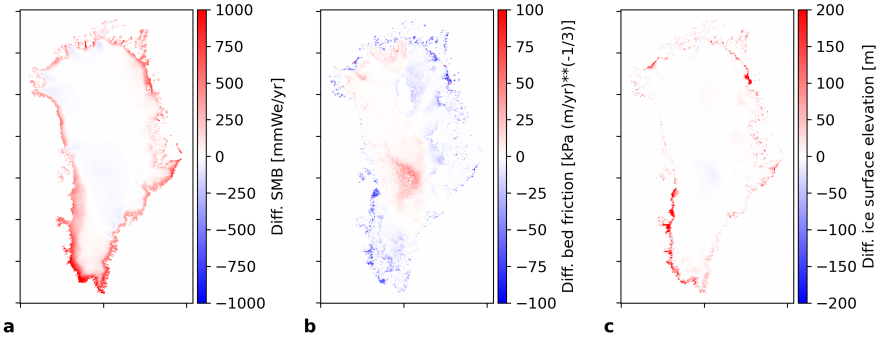

Figure 2. Differences between the initialization with NorESM2-MM and the initialization with ERA5 after relaxation: SMB (a), friction parameter (b) and ice surface elevation (c).

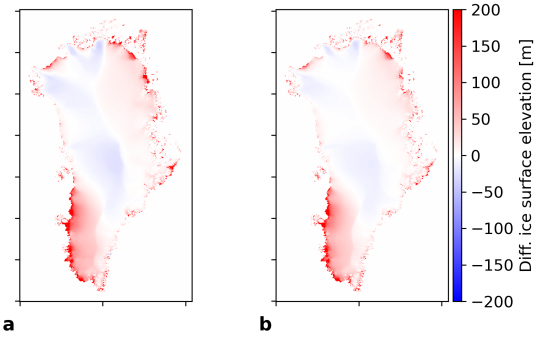

Figure 3. Comparison of differences in ice surface elevation to the ERA5-initialization after the 1000 year relaxation for different initialization strategies using ERA5-SMB and NorESM2-MM-SMB. For detailed explanation see main text.

each other. This indicates that the ice sheet geometry before relaxation, which is slightly different in both cases, is not the decisive factor for the resulting ice sheet geometry. It is rather the mismatch between SMB and friction field that leads to a deviation from the ERA5-initialization. The mismatch between SMB and friction field results in a build up of the ice sheet where higher friction prevents efficient evacuation of excess ice, while it leads to a thinning of the ice sheet in areas where low friction inhibits ice sheet growth. Differences are prominent in the same regions where differences in ice surface elevation between the NorESM2-MM and the ERA5-initialization are pronounced, e. g. at the South-West margins of the ice sheet, as well as in distinct areas of the North margin (Fig. 3 c). This demonstrates how a mismatch between SMB and friction field would propagate into a biased ice sheet geometry in the absence of further calibration.

https://doi.org/10.5194/egusphere-2024-922
Preprint. Discussion started: 29 April 2024

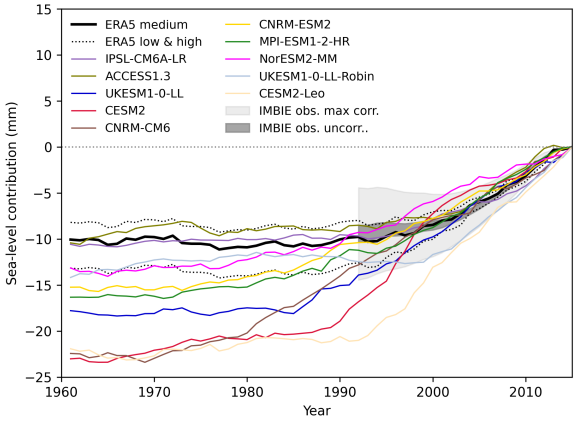

Figure 4. Sea-level contribution over the historical period relative to 2015. Grey shadings show envelopes of observed mass loss (Shepherd et al., 2020) for which either a maximal error correlation (light grey shading), or uncorrelated errors (dark grey shading) are assumed. Note that, in this case, we calculate sea-level contribution omitting correction for density to use the same units of IMBIE observations. The ESM-initialized simulations (colored lines) are only shown for medium sensitivity to outlet-glacier retreat forcing, while we display all sensitivities for the ERA5-forced simulations (black lines).

3.2 Historical period

In all simulations the ice sheet loses mass over the historical period, although at different rates. In terms of sea-level contribution relative to 2015, the ensemble of ESM-initialized simulations match the observations fairly well (Fig. 4b). The increased mass loss of the ice sheet starting in the 1990s is captured by all members. However, onset and slope differ between simulations, which can be attributed to the fact that the ESM forcing does not reproduce the observed interannual and interdecadal variability. Runs initialized and forced with ERA5-reanalysis data closely agree with observations, which we attribute to the realistic replication of interannual and interdecadal variability in the forcing. This applies in particular to runs where medium sensitivity to outlet-glacier retreat forcing is applied.

Considering the good match with observations of the historical ERA5 run with medium sensitivity to outlet glacier retreat forcing, we focus our presentation of results on this parameter choice.

3.3 Projections

After performing historical simulations, we carry out unforced control experiments, for which the SMB and ST anomalies are set to 0. The control projections yield a sea-level contribution ranging from 2.3 to 7.3 mm by the year 2100. This minor contribution can mainly be attributed to drift induced by historical forcing, while a minor part is due to residual drift originating in the initialization. Throughout the historical simulations, the ice sheet experiences increasingly negative SMB forcing,

https://doi.org/10.5194/egusphere-2024-922
Preprint. Discussion started: 29 April 2024

including inter annual variability. Given the strong agreement of the historical runs with observations, we justify utilizing the projections without subtracting an unforced control experiment, marking a notable improvement over previous experiments, e.g. such as those performed in ISMIP6 (Goelzer et al., 2020b).

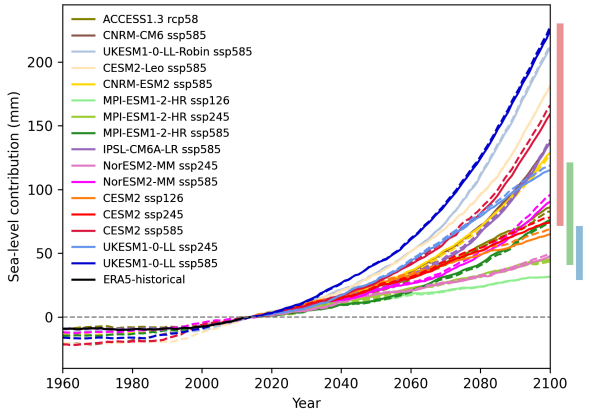

Figure 5. Projected sea-level contributions relative to 2015. Solid lines are projections starting from the ERA5-initialization, dashed lines are projections that were initialized with the ESM-own SMB. All simulations were run with medium sensitivity to outlet-glacier retreat forcing. Vertical bars denote the range of projected sea-level contribution per scenario: SSP5-8.5 (red), SSP2-4.5 (green), SSP1-2.6 (blue).

Sea-level contribution increases under all scenarios (Fig. 5), indicating progressive mass loss of the ice sheet. While for the low and intermediate emission scenarios (SSP1-2.6 and SSP2-4.5) the increase in sea-level contribution is almost linear over the entire century, mass loss accelerates significantly under the high emission scenario (SSP5-8.5) towards the end of the century. Average rates of change under SSP1-2.6 are $0.7\,\mathrm{mm\ yr^{-1}}$ for the period 2040-2050 and $0.6\,\mathrm{mm\ yr^{-1}}$ for the period 2090-2100, which is similar to present day observations (Rignot et al., 2008; Shepherd et al., 2012). For the SSP2-4.5 scenario rates of change amount to $0.8\,\mathrm{mm\ yr^{-1}}$ over the period 2040-2050 and $1.1\,\mathrm{mm\ yr^{-1}}$ over the period 2090-2100, respectively. In contrast, SSP5-8.5 forced projections exhibit a rate of change of $0.9\,\mathrm{mm\ yr^{-1}}$ over the period 2040-2050, which increases to $3.7\,\mathrm{mm\ yr^{-1}}$ over the period 2090-2100. Taking the year 2015 as reference, the total sea-level contribution by 2100 is projected to be between 32 and 69 mm for the low emission scenario and between 44 and 119 mm (74 and 228 mm) for the intermediate (high) emission scenario, respectively. The ensemble shows a notable overlap of the intermediate scenario with the low and the high emission scenario, demonstrating high uncertainty in the projections stemming from the climate forcing. This uncertainty is most pronounced for the SSP5-8.5 scenario, where the range of projected sea-level contribution amounts to 154 mm. The highest contribution of the entire ensemble comes from the UKESM1-0-LL-SSP5-8.5 forced projection, while the lowest contribution in the SSP5-8.5 group (forced with MPI-ESM1-2-HR) is almost as low as the highest contribution in the SSP1-2.6 group (forced with CESM2). Detailed results for all projections are given in Table A1.

https://doi.org/10.5194/egusphere-2024-922
Preprint. Discussion started: 29 April 2024

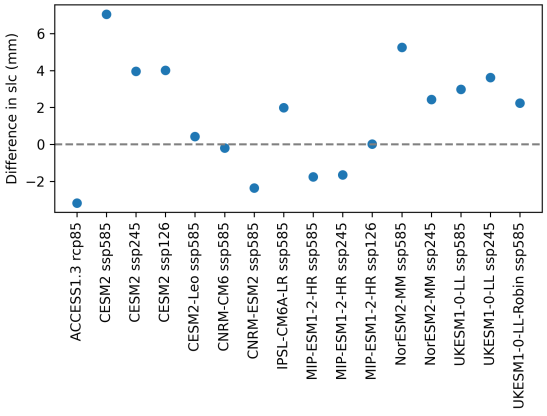

Figure 6. Differences in sea-level contribution until 2100 for projections starting from an ESM-initial state vs starting from an ERA5-initial states.

Differences in sea-level contribution originating from different initializations (ESM-init vs. ERA5-init) are rather small compared to the ensemble spread due to climate forcing. At the end of 2100 projections initialized with ESM forcing deviate from their respective ERA-initialized projections by -3.2 mm to +7.1 mm (Fig. 6), which is equivalent to -4.1% to 6.6% relative to the total contribution. There is no clear trend as to whether the ESM-initialized projections over- or underestimate sea-level contributions relative to their ERA5-initialized counter parts. The mean absolute difference is only 2.7 mm (equivalent to 2.9%), implying a relatively low impact of the forcing used for initialization and the resulting friction field on the projections for the used modeling strategy.

To further asses the impact of the initial ice sheet state on the resulting sea-level contribution in the year 2100, we analyze how various state parameters of the initial ice sheet (SMB, bed friction and ice sheet thickness) relate to differences in sea-level contribution in the year 2100 (Fig. 7a-c). All parameters are spatially integrated around the margins of the ice sheet where differences in ice sheet thickness to the ERA5-initialized ice sheet and changes during projection are most pronounced. This is done by selecting grid cells where the horizontal ice velocities at the surface of the ERA5-initialized ice sheet exceed $50\,\mathrm{m\,yr^{-1}}$ (Fig. 7d). We fit the relative differences in SMB, friction parameter and ice thickness of the initialized ice sheets (ESM-initialization - ERA5-initialization) to the relative differences in projected sea-level contribution of the corresponding projections (ESM-initialized - corresponding ERA5-initialized) using a linear regression. While bedrock friction (Fig. 7b) shows only weak linear relationship to projected sea-level contribution, initial SMB (Fig. 7a) and ice thickness (Fig. 7c) exhibit strong linear relationship to projected sea-level contribution. Projections that initially start with relatively thicker ice sheet margins tend to yield higher sea-level contributions. This is a result from higher SMB at the margins provided by the "biased" ESMs during the spin-up period. As the inversion is unable to completely counteract the build up of thick margins, a residual remains after the initialization is complete. Therefore, those initial ice sheets have more mass at their margins available for removal by run-off and retreat of outlet glaciers when the same anomalous forcing is applied, which leads to higher mass loss.

https://doi.org/10.5194/egusphere-2024-922
Preprint. Discussion started: 29 April 2024

This effect is further promoted by lower friction around the margins, which is a result of the inversion process, as the model is trying to compensate for too thick ice.

280

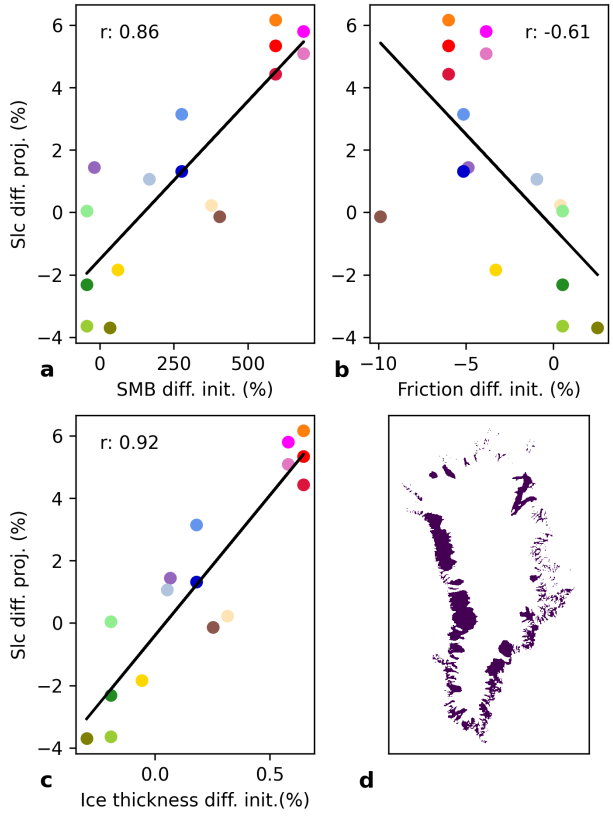

Figure 7. Relative differences in sea-level contribution by 2100 vs. relative differences in filtered and spatially integrated SMB (a), friction coefficient (b) ice thickness (c) after ice sheet initalization. Black lines in a-c denote linear fits. Correlation coefficients as a measure of the goodness of the fit are given within each panel. The color scheme is the same as in Fig. 5. d shows the masked area of the ERA5-initialization where surface velocities are lager than $50\,\mathrm{m\,yr^{-1}}$. The mask is used to chose areas over which SMB, friction coefficient and ice thickness of each ESM-initialization are integrated and compared against the ERA5-initialization. Note that the analysis has been proven robust to variations in the filter velocity, as similar results have been found with different velocity filters ($30\,\mathrm{m\,yr^{-1}}$ – $80\,\mathrm{m\,yr^{-1}}$), as long as the filtered area represents the margin of the ice sheet. For detailed description see main text.

To sample uncertainty in the outlet-glacier retreat parameterization, all simulations are run with three different sensitivities to outlet-glacier retreat forcing (Slater et al., 2020). We compare sea-level contributions for all three emission scenarios (Fig. 8). The mean spread in sea-level contribution due to outlet-glacier retreat forcing for the projections forced with the low emission scenario is $5\,\mathrm{mm}$. For projections forced with the intermediate emission scenario the mean spread amounts to $11\,\mathrm{mm}$, while

https://doi.org/10.5194/egusphere-2024-922
Preprint. Discussion started: 29 April 2024

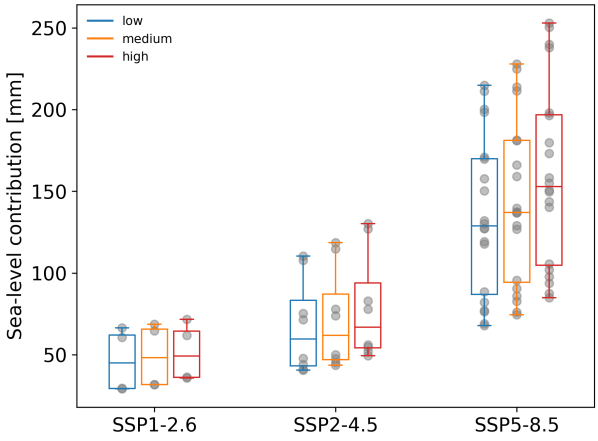

Figure 8. Projected sea-level contribution until 2100 for the entire ensemble, grouped by emission scenario. Colors denote sensitivity to outlet-glacier retreat forcing. Grey dots represent the individual ESM-projections, which include results for both initialization methods.

the mean spread increases to 25 mm for projections forced with the high emission scenario.

3.3.1 Mass loss contribution from SMB vs outlet-glacier discharge

We examine the relative importance of SMB forcing vs outlet-glacier retreat forcing by analyzing additional experiments where only part of the forcing is activated at a time. Supplementary to the ERA5-initialized fully-forced projections we carry out three additional experiments: An SMB-only experiment, where outlet-glacier retreat forcing is switched off, a Retreat-only experiment, where no SMB anomalies are prescribed, and a No-SMB-height-feedback experiment, where all forcings are activated, except for the SMB-height feedback.

Sea-level contribution for the NorESM-MM-SSP5-8.5 projection steeply increases over the second half of the century in the fully forced experiment, as well as in the SMB-only and the No-SMB-height-feedback experiment (Fig. 9). In contrast, sea-level contribution remains almost linear when only outlet-glacier retreat forcing is applied, which signifies an increasingly important role of SMB for future mass loss processes of the ice sheet under the high emission scenario. The response of the ice sheet to this high emission scenario is dominated by an increasingly negative SMB, which causes mass loss to accelerate around the margins of the ice sheet.

Spatial patterns of mass loss for the fully forced, as well as the partially forced experiments are illustrated in Fig. 11 for the NorESM2-MM-SSP58-5.8 projection. The SMB-driven thinning of the margin is especially pronounced in the South-West of Greenland. The contribution to the total mass loss by outlet glaciers is most prominent in the North-West, the North and parts of the East of the ice sheet, while the SMB-height feedback affects the ice sheet mostly around the margins, where mass loss

https://doi.org/10.5194/egusphere-2024-922
Preprint. Discussion started: 29 April 2024

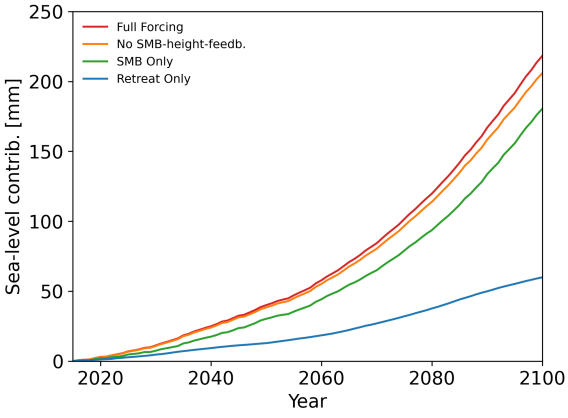

Figure 9. Projected sea-level contribution relative to 2015 for the NorESM2-MM-SSP5-8.5 run with full forcing (red line), without SMB-height feedback (orange line), with SMB forcing only (green line) and with outlet-glacier retreat forcing only (blue). All experiments where retreat forcing is switched on use a medium sensitivity to outlet-glacier retreat forcing.

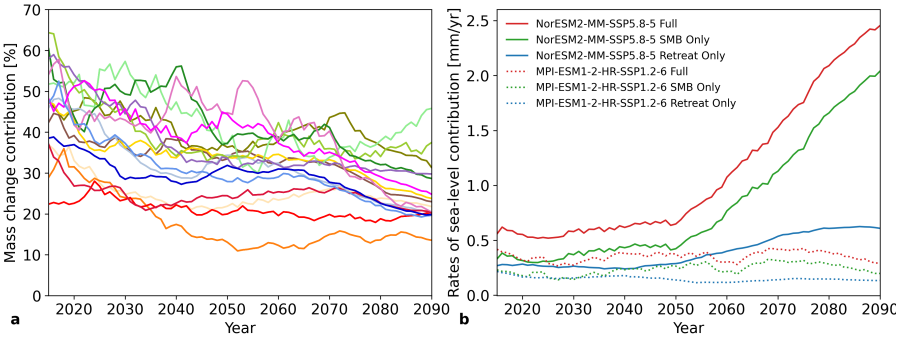

Figure 10. Estimates of relative importance of outlet-glacier retreat forcing relative to the fully forced experiments, calculated as the ratio of 20-year running mean annual sea-level contribution rates of the Retreat-only experiments to the respective fully forced experiments (a). Color scheme is the same as in Fig. 5. The prominent variability is mainly caused by high variability in the SMB forcing. Note that the the combination of both mass change mechanisms exceeds 100% (for detailed explanation see main text). Partitioning of rates of sea-level contribution for the fully forced experiment (red), the SMB-Only experiment (green) and the Retreat-only experiment for two exemplary ESM-SSP combinations: NorESM2-MM-SSP5-8.5 (solid lines) and MPI-ESM1-2-HR-SSP1-2.6 (dashed lines) (b).

occurs as as combination of SMB-induced thinning and dynamic thinning driven by outlet glacier retreat. In the fully forced
305 experiment, both mechanisms compete for their role in mass loss partially intensifying and mitigating each other. Retreat of outlet-glaciers leads to a dynamic acceleration of ice flow from regions inland down to lower elevations, where surface melt intensifies, while at the same time the SMB-induced ablation upstream counteracts the effective removal of ice via discharge

https://doi.org/10.5194/egusphere-2024-922
Preprint. Discussion started: 29 April 2024

via the outlet glaciers.

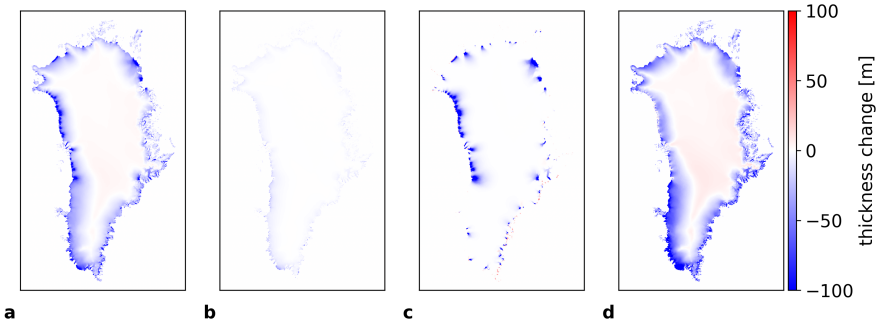

Figure 11. Ice thickness change (2100-2015) in the fully forced experiment of the NorESM2-MM-SSP58-5.8 projection (a). Residual of ice thickness change of the full experiment minus the partially forced experiments: full forcing experiment - no-SMB-height feedback experiment (b), full forcing experiment - SMB-only experiment (c), full forcing experiment - Retreat-only experiment (d).

Table1 gives a full overview of the relative importance of each forcing mechanism for the entire ensemble. Until 2100 the SMB-only projections for the SSP5-8.5 scenario yield 78±5 % relative to the respective fully forced experiments, while the Retreat-only experiments contribute only 31±5 % compared to the full experiments. Notably, the sum of the SMB-only and the Retreat-only experiments exceed the contribution of the fully forced experiments by ca. 9 %. When both forcings are active, this residual is compensated by progressive SMB-induced thinning of the margins, which consequently reduces the amount of ice mass available for removal by outlet-glacier discharge. At the same time, when the ablation area is reduced by the outlet-glacier discharge, this area is no longer available for negative SMB to be effective on it. The resulting sea-level contribution in the fully forced experiment is thus no linear combination of the results in the SMB-only and the Retreat-only experiments.

The relative importance of discharge from outlet-glaciers for the the mass loss of the ice sheet decreases over the century for almost all experiments (Fig. 10a). This is mainly driven by a growing contribution from the decreasing SMB. Rates of sea-level contribution steeply increase in the SMB-only high emission experiments, while corresponding rates of sea-level contribution from the Retreat-only experiments only increase slightly during the second half of the century, before flattening at the end of the century (Fig. 10b). Warm waters from the ocean in combination with increased runoff from the ice sheet at the glacier terminus cause accelerated retreat of outlet-glaciers. This process decelerates and ultimately succumbs when the presently marine-terminating glaciers partially run aground on land and hence lose contact with the ocean. Exceptions are the low and the medium emission scenario of the MPI-ESM1-2-HR run, where SMB increases at the end of the century, causing a reduction in the relative contribution from the rather stable rates of sea-level contribution generated by the retreat of outlet glaciers.

https://doi.org/10.5194/egusphere-2024-922
Preprint. Discussion started: 29 April 2024

Table 1. Sea-level contribution until 2100 for partially forced projections relative to the fully forced experiment.

Scenario	SMB-only [%]	Retreat sens.	Retreat-only [%]	SMB-height-feedb. [%]
SSP1-2.6	77±11	low	24±13	8±1
		medium	31±13	8±1
		high	32±19	8±0
SSP2-4.5	76±8	low	27±7	7±0
		medium	32±8	7±0
		high	40±10	7±0
SSP5-8.5	78±5	low	24±5	6±1
		medium	31±5	5±1
		high	40±6	5±1

On the considered time scale, the SMB-height feedback plays a significantly smaller role, when compared to the other mechanisms. It does, however, increasingly gain in importance, as the ice sheet geometry progressively changes in response to an increasingly negative SMB. While the sea-level contributions of the No-SMB-height feedback experiments under the SSP5-8.5 scenario are almost equivalent to the fully forced experiment during the first half of the century (Fig. 9), the difference increases to 5±1 % by 2100. Notably, different sensitivities to the retreat forcing do not significantly impact the relative contribution from the SMB-height-feedback. This is because the area where the effect is active is not reduced, but merely shifted inland by a progressive retreat of the outlet glaciers.

4 Discussion and conclusions

In this study we present ensemble projections of sea-level contribution from the Greenland ice sheet over the 21st century under three emission scenarios using regionally downscaled forcing from various ESMs of the CMIP6 archive. We investigate the impact of forcing used for initialization on the projected sea-level contribution and analyze the relative importance of SMB forcing, outlet-glacier retreat forcing and SMB-height feedback on the projections. Our simulations yield a sea-level contribution of 30 to 70 mm under the SSP1-2.6 scenario, 40 to 120 mm under the SSP2-4.5 and 70 to 230 mm under the SSP5-8.5 scenario. These numbers exceed sea-level projections reported by Goelzer et al. (2020b) in the ISMIP6 project (32±17 mm for RCP2.6 and 90±50 mm for RCP8.5), which used forcing for only two emission scenarios and sampled fewer ESMs from the CMIP5 archive, but used a number of different ice sheet models. Our numbers are, however, comparable to studies that used CMIP6 forcing (Hofer et al., 2020; Payne et al., 2021; Choi et al., 2021).

https://doi.org/10.5194/egusphere-2024-922
Preprint. Discussion started: 29 April 2024

The relative importance of SMB vs outlet glacier retreat in future mass loss of the Greenland ice sheet is highly uncertain, mainly due to the fact that processes responsible for outlet glacier retreat are insufficiently understood and difficult to model. Our simulations suggest an increasing importance of SMB over mass loss from outlet-glaciers in the future evolution of the ice sheet. This result is generally in line with findings by Fürst et al. (2015), although their study indicates an even larger relative contribution from SMB over oceanic forcing until 2100, especially for the higher emission scenarios. In contrast to our findings, Choi et al. (2021), who estimate melt rates at the glacier fronts using and undercutting parameterization, argue that, under SSP5-8.5, the contribution of outlet glacier retreat to mass loss from the ice sheet will be as high as 56% by the end of the century. The large discrepancy in estimates can possibly be explained by the different periods used for tuning of the respective retreat parameterizations. While Choi et al. (2021) calibrate their calving parameterization over a relatively recent period of 11 years, where observed glacier retreat was faster than over the period of 1960 to 2018, which was used to calibrate the retreat parameterization used in this study.

Uncertainty analysis of our ensemble shows that climate forcing constitutes the largest source of uncertainty for projected sea-level contribution. With a spread of 154 mm for the SSP5-8.5 scenario, 75 mm for the SSP2-4.5 scenario and 37 mm for the SSP1-2.6 scenario, and a significant overlap across scenarios, uncertainty in projected sea-level rise due to climate forcing exceeds any of the other sampled uncertainties. This range of uncertainty is notably larger than the uncertainty due to ice sheet model, as evaluated in the ISMIP6 study. Goelzer et al. (2020b) reported a spread of about 80 mm in projections for the high emission scenario stemming from the different ice sheet models. This spread is smaller than the uncertainty we attribute to climate forcing, which indicates a larger relative importance of the boundary conditions over the ice sheet model formulations and the characteristics of the set-up, as well as specific modeling choices.

The uncertainty in SMB can largely be attributed to climate forcing uncertainty, as shown by previous studies (Holube et al., 2022). However, another significant uncertainty in projected sea-level contribution stems from the uncertainty in the parameterization for outlet-glacier retreat, which amounts to a spread of up to 25 mm in the projections. While we find the initial state of the ice sheet (SMB, friction field and ice sheet thickness) to have an impact on the projected mass loss, with an uncertainty of less than 10 mm this impact remains small. The mean spread of sea-level contribution until 2100 due to grid spacing is 2.8 mm, indicating a similarly low dependency of results on grid size. This can be attributed to the near grid-size independent formulation of the outlet-glacier retreat parameterization as well as the conservative interpolation of SMB forcing.

Goelzer et al. (2020b) identified improvements on initialization techniques to minimize inaccuracies in the initial state of the ice sheet as a key priority for the ice sheet modeling community. In the ISMIP6 study a good match of initial ice sheet geometry (or surface velocity) with observations often coincided with a large model drift after the initialization. In the present study, we progress on that matter by presenting an initialization, along with a historical run, that matches well with observations and avoids large model drifts at the same time. We regard this as an important step forward when it comes to modeling frameworks for future ice sheet intercomparison projects. A drawback of the inversion method used in this study is that it leads to a nonphysical transfer of uncertainties, such as SMB and model parameter uncertainty, into the bed friction field. In lack of available observational data of accurate bedrock conditions underneath the ice, this is, however, an acceptable approach, since it has limited effects on a centennial timescale.

https://doi.org/10.5194/egusphere-2024-922
Preprint. Discussion started: 29 April 2024

The residual drift observed in the control experiments following the historical run could typically be interpreted as the committed sea-level contribution by 2015. However, because SMB and ST anomalies are reset to 0 after 2015, the control forcing does not reflect the recent forcing experienced by the ice sheet. Instead, the forcing is returned to a 1960-1989-mean, which is a period of assumed steady state of the ice sheet. This means, that the control experiments only offer insight into how the ice sheet reacts to short-term perturbations from this assumed steady state, rather than providing conclusive information about its future response to historical forcing. To accurately estimate the committed sea-level contribution by 2015, it would be necessary to force the control projections with constant values from that year. However, the considerable interannual variability makes it difficult to adequately represent the recent observed mass loss of the ice sheet when continuously applying forcing from a single specific year. Alternative methods to determine the committed sea-level contribution could include using the mean over a certain time span from the recent period to better reflect the recently observed negative mass trend.

The ISMIP6 forcing approach made use of SMB anomalies, to remove ESM and RCM biases and to provide an experimental setup suitable for ensemble projections. However, ISMIP6 identified the need to explore a more consistent forcing approach, with full SMB fields. In this study, we assess this issue by comparing projections utilizing both SMB anomalies and absolute SMB. We employ two simulation strategies: one initializing the ice sheet with ESM-based SMB and forcing subsequent projections with absolute SMB from the ESM; the other combining the baseline SMB used for initialization with ESM-SMB anomalies to its own baseline SMB. In both cases the anomalies are the same, which makes the projections directly comparable. Our results show that there is little to no difference in the projected sea-level contribution when comparing the two approaches. This suggests that the choice between using an SMB product from reanalysis or SMB from an ESM for initialization does not significantly impact the uncertainties in the projections. Furthermore, our result confirm that a modeling setup that uses a common initialization and forces the projections with anomalies is suitable for large ensembles of ice sheet projections. This is especially relevant for community efforts that rely on a common modeling setup, such as future intercomparison projects.

While we use forcing from a number of ESMs, we consider only one RCM (MAR), thereby neglecting to sample RCM uncertainty. Considering the increasing importance of SMB for future mass loss processes of the ice sheet and the relatively large discrepancies in modeled SMB between different RCMs (Glaude et al. in preparation), it is desirable to include the RCM uncertainty in future studies. Another restriction of this study is the fact that only one ice sheet model is used. Hence, uncertainties stemming from model formulation, parameter uncertainty, as well as modeler's choices are not reflected here.

While many past studies have focused their attention on the two extreme ends of emission scenarios (the SSP1-2.6 and the SSP5-8.5), we succeed to close this gap in scenario uncertainty, by including multiple projections for the intermediate SSP2-4.5 scenario. In light of current socioeconomic conditions, the SSP2-4.5 might be a particularly realistic future pathway and it is therefore important to increasingly sample projections for this scenario.

The strength of the parameterization used in this study to represent retreat of marine terminating outlet-glaciers in response to ocean warming is its independence from model resolution and its empirically based nature. An advantageous consequence of this is, that projections of sea-level contribution are largely independent of grid resolution. As demonstrated in this study, a coarser grid resolution (e.g. 16 km) proves to be sufficient, which is crucial when it comes to the efficient use of computational resources. This becomes relevant when running large ensembles of projections, for example, when sampling a wide range of

https://doi.org/10.5194/egusphere-2024-922
Preprint. Discussion started: 29 April 2024

climate forcing or when exploring parameter uncertainty. The parameterization's inability to resolve individual outlet glaciers and, in particular, fjord bathymetry is, however, a significant weakness, as this inhibits the representation small scale processes in fjords and at the glacier front which are important drivers for the retreat of outlet-glaciers. Future efforts are needed to improve on the representation of processes at the ocean-ice interface, especially with the prospect of accurate sea-level projections beyond 2100.

Further progression on the improvement of accurate projections of sea-level contribution by the Greenland ice sheet rely on the ongoing collaboration of research teams across the field, including intensified efforts to integrate results from modeling with observations.

Code and data availability. CMIP6 data are freely available from the Earth System Grid Federation at https://esgf.llnl.gov. The CISM code is freely available at https://github.com/CISM. The model output will be made available upon acceptance at the Sigma2 Research Data Archive (NIRD RDA) at https://archive.sigma2.no. Scripts used for the analysis in this study are available upon request from the corresponding author.

Author contributions. HG contributed to the design of the study, as well as to the discussion of results, and supervised the work. CR performed all experiments and analyzed the results. The manuscript was written by CR with input and critical feedback from all authors.

Competing interests. The authors declare that they have no conflict of interest.

Financial support. CR and HG have received funding from the Research Council of Norway under project 324639. HG has received funding from the European Union's Horizon 2020 Research and Innovation Programme under grant agreement no. 869304, PROTECT.

Acknowledgements. We acknowledge Xavier Fettweis and the MAR group for providing regionally downscaled climate forcing. High-performance computing and storage resources were provided by Sigma2 - the National Infrastructure for High Performance Computing and Data Storage in Norway through projects NN8006K, NN8085K, NS8006K, NS8085K and NS5011K. This is PROTECT publication number (to be determined when accepted).

We acknowledge the World Climate Research Programme (WCRP) and its Working Group on Coupled Modelling for coordinating and promoting CMIP6. We thank the climate modeling groups for producing and making available their model output, and the Earth System Grid Federation (ESGF) for archiving the CMIP data and providing access.

https://doi.org/10.5194/egusphere-2024-922
Preprint. Discussion started: 29 April 2024

The authors would like to emphasize that the findings of this study are to be regarded as a continuation of ongoing community effort and would not be possible without previous work and the provision of data by many different sources.

Appendix A

Table A1. Sea-level contributions for projections run on 4 km grid resolution. Listed are projections initialized with ERA5 (ESM) SMB. Low, med and high denote the sensitivity to outlet-glacier retreat forcing.

ESM-SSP projection	Sea-level contrib. until 2050 [mm]			Sea-level contrib. until 2100 [mm]		
	low	med	high	low	med	high
ACCESS1.3-ssp585	21 (20)	22 (21)	25 (24)	77 (76)	86 (83)	98 (94)
CNRM-CM6-ssp585	25 (23)	26 (25)	30 (28)	127 (127)	137 (137)	151 (150)
UKESM1-0-LL-Robin-ssp585	35 (35)	38 (38)	41 (42)	198 (200)	211 (214)	238 (240)
CESM2-Leo-ssp585	34 (34)	36 (36)	39 (39)	170 (171)	181 (181)	196 (198)
CNRM-ESM2-ssp585	24 (23)	26 (24)	30 (28)	119 (118)	129 (127)	144 (140)
MPI-ESM1-2-HR-ssp126	12 (12)	14 (13)	16 (15)	29 (30)	32 (32)	36 (36)
MPI-ESM1-2-HR-ssp245	16 (15)	18 (16)	21 (18)	41 (41)	45 (44)	52 (49)
MPI-ESM1-2-HR-ssp585	13 (12)	14 (13)	17 (15)	69 (68)	76 (74)	87 (85)
IPSL-CM6A-LR-ssp585	22 (23)	22 (24)	24 (27)	130 (132)	137 (140)	155 (158)
NorESM2-ssp245	17 (19)	18 (19)	21 (21)	44 (48)	48 (50)	55 (56)
NorESM2-ssp585	20 (21)	22 (23)	26 (25)	82 (89)	90 (96)	102 (106)
CESM2-CMIP6-ssp126	23 (27)	27 (28)	24 (30)	61 (66)	65 (69)	62 (72)
CESM2-CMIP6-ssp245	25 (26)	25 (26)	26 (28)	72 (75)	74 (78)	78 (83)
CESM2-CMIP6-ssp585	29 (30)	30 (31)	32 (33)	151 (158)	159 (166)	173 (180)
UKESM1-0-LL-CMIP6-ssp245	29 (29)	31 (32)	35 (36)	108 (110)	115 (119)	127 (130)
UKESM1-0-LL-CMIP6-ssp585	42 (42)	44 (45)	49 (49)	211 (215)	225 (228)	250 (253)

https://doi.org/10.5194/egusphere-2024-922
Preprint. Discussion started: 29 April 2024

References

Adalgeirsdóttir, G., Aschwanden, A., Khroulev, C., Boberg, F., Mottram, R., Lucas-Picher, P., and Christensen, J. H.: Role of model initialization for projections of 21st-century Greenland ice sheet mass loss, Journal of Glaciology, 60, https://doi.org/10.3189/2014JoG13J202, 2014.

Aschwanden, A., Aøalgeirsdóttir, G., and Khroulev, C.: Hindcasting to measure ice sheet model sensitivity to initial states, Cryosphere, 7, https://doi.org/10.5194/tc-7-1083-2013, 2013.

Berends, C. J., Wal, R. S. V. D., Akker, T. V. D., and Lipscomb, W. H.: Compensating errors in inversions for subglacial bed roughness: same steady state, different dynamic response, Cryosphere, 17, https://doi.org/10.5194/tc-17-1585-2023, 2023.

Bindschadler, R. A., Nowicki, S., Abe-OUCHI, A., Aschwanden, A., Choi, H., Fastook, J., Granzow, G., Greve, R., Gutowski, G., Herzfeld, U., Jackson, C., Johnson, J., Khroulev, C., Levermann, A., Lipscomb, W. H., Martin, M. A., Morlighem, M., Parizek, B. R., Pollard, D., Price, S. F., Ren, D., Saito, F., Sato, T., Seddik, H., Seroussi, H., Takahashi, K., Walker, R., and Wang, W. L.: Ice-sheet model sensitivities to environmental forcing and their use in projecting future sea level (the SeaRISE project), Journal of Glaciology, 59, https://doi.org/10.3189/2013JoG12J125, 2013.

Brinkerhoff, D. J. and Johnson, J. V.: Data assimilation and prognostic whole ice sheet modelling with the variationally derived, higher order, open source, and fully parallel ice sheet model VarGlaS, Cryosphere, 7, https://doi.org/10.5194/tc-7-1161-2013, 2013.

Broeke, M. V. D., Bamber, J., Ettema, J., Rignot, E., Schrama, E., Berg, W. J. D. V., Meijgaard, E. V., Velicogna, I., and Wouters, B.: Partitioning recent Greenland mass loss, Science, 326, https://doi.org/10.1126/science.1178176, 2009.

Choi, Y., Morlighem, M., Rignot, E., and Wood, M.: Ice dynamics will remain a primary driver of Greenland ice sheet mass loss over the next century, Communications Earth and Environment, 2, https://doi.org/10.1038/s43247-021-00092-z, 2021.

Edwards, T. L., Fettweis, X., Gagliardini, O., Gillet-Chaulet, F., Goelzer, H., Gregory, J. M., Hoffman, M., Huybrechts, P., Payne, A. J., Perego, M., Price, S., Quiquet, A., and Ritz, C.: Effect of uncertainty in surface mass balance-elevation feedback on projections of the future sea level contribution of the Greenland ice sheet, Cryosphere, 8, https://doi.org/10.5194/tc-8-195-2014, 2014.

Enderlin, E. M., Howat, I. M., Jeong, S., Noh, M. J., Angelen, J. H. V., and Broeke, M. R. V. D.: An improved mass budget for the Greenland ice sheet, Geophysical Research Letters, 41, https://doi.org/10.1002/2013GL059010, 2014.

Eyring, V., Bony, S., Meehl, G. A., Senior, C. A., Stevens, B., Stouffer, R. J., and Taylor, K. E.: Overview of the Coupled Model Intercomparison Project Phase 6 (CMIP6) experimental design and organization, Geoscientific Model Development, 9, https://doi.org/10.5194/gmd-9-1937-2016, 2016.

Fettweis, X., Box, J. E., Agosta, C., Amory, C., Kittel, C., Lang, C., As, D. V., Machguth, H., and Gallée, H.: Reconstructions of the 1900-2015 Greenland ice sheet surface mass balance using the regional climate MAR model, Cryosphere, 11, https://doi.org/10.5194/tc-11-1015-2017, 2017.

Fürst, J. J., Goelzer, H., and Huybrechts, P.: Ice-dynamic projections of the Greenland ice sheet in response to atmospheric and oceanic warming, Cryosphere, 9, https://doi.org/10.5194/tc-9-1039-2015, 2015.

Gillet-Chaulet, F., Gagliardini, O., Seddik, H., Nodet, M., Durand, G., Ritz, C., Zwinger, T., Greve, R., and Vaughan, D. G.: Greenland ice sheet contribution to sea-level rise from a new-generation ice-sheet model, Cryosphere, 6, https://doi.org/10.5194/tc-6-1561-2012, 2012.

Gillet-Chaulet, F., Durand, G., Gagliardini, O., Mosbeux, C., Mouginot, J., Rémy, F., and Ritz, C.: Assimilation of surface velocities acquired between 1996 and 2010 to constrain the form of the basal friction law under Pine Island Glacier, Geophysical Research Letters, 43, https://doi.org/10.1002/2016GL069937, 2016.

https://doi.org/10.5194/egusphere-2024-922
Preprint. Discussion started: 29 April 2024

Goelzer, H., Huybrechts, P., Fürst, J. J., Nick, F. M., Andersen, M. L., Edwards, T. L., Fettweis, X., Payne, A. J., and Shannon, S.: Sensitivity of Greenland ice sheet projections to model formulations, Journal of Glaciology, 59, https://doi.org/10.3189/2013JoG12J182, 2013.

Goelzer, H., Nowicki, S., Edwards, T., Beckley, M., Abe-Ouchi, A., Aschwanden, A., Calov, R., Gagliardini, O., Gillet-Chaulet, F., Golledge, N. R., Gregory, J., Greve, R., Humbert, A., Huybrechts, P., Kennedy, J. H., Larour, E., Lipscomb, W. H., Leclech, S., Lee, V., Morlighem, M., Pattyn, F., Payne, A. J., Rodehacke, C., Rückamp, M., Saito, F., Schlegel, N., Seroussi, H., Shepherd, A., Sun, S., Wal, R. V. D., and Ziemen, F. A.: Design and results of the ice sheet model initialisation initMIP-Greenland: An ISMIP6 intercomparison, Cryosphere, 12, https://doi.org/10.5194/tc-12-1433-2018, 2018.

Goelzer, H., Coulon, V., Pattyn, F., Boer, B. D., and Wal, R. V. D.: Brief communication: On calculating the sea-level contribution in marine ice-sheet models, Cryosphere, 14, https://doi.org/10.5194/tc-14-833-2020, 2020a.

Goelzer, H., Nowicki, S., Payne, A., Larour, E., Seroussi, H., Lipscomb, W. H., Gregory, J., Abe-Ouchi, A., Shepherd, A., Simon, E., Agosta, C., Alexander, P., Aschwanden, A., Barthel, A., Calov, R., Chambers, C., Choi, Y., Cuzzone, J., Dumas, C., Edwards, T., Felikson, D., Fettweis, X., Golledge, N. R., Greve, R., Humbert, A., Huybrechts, P., Clec'H, S. L., Lee, V., Leguy, G., Little, C., Lowry, D., Morlighem, M., Nias, I., Quiquet, A., Rückamp, M., Schlegel, N. J., Slater, D. A., Smith, R., Straneo, F., Tarasov, L., Wal, R. V. D., and Broeke, M. V. D.: The future sea-level contribution of the Greenland ice sheet: A multi-model ensemble study of ISMIP6, Cryosphere, 14, https://doi.org/10.5194/tc-14-3071-2020, 2020b.

Goldberg, D. N.: A variationally derived, depth-integrated approximation to a higher-order glaciological flow model, Journal of Glaciology, 57, https://doi.org/10.3189/002214311795306763, 2011.

Good, S. A., Martin, M. J., and Rayner, N. A.: EN4: Quality controlled ocean temperature and salinity profiles and monthly objective analyses with uncertainty estimates, Journal of Geophysical Research: Oceans, 118, https://doi.org/10.1002/2013JC009067, 2013.

Gregory, J. M., Griffies, S. M., Hughes, C. W., Lowe, J. A., Church, J. A., Fukimori, I., Gomez, N., Kopp, R. E., Landerer, F., Cozannet, G. L., Ponte, R. M., Stammer, D., Tamisiea, M. E., and van de Wal, R. S.: Concepts and Terminology for Sea Level: Mean, Variability and Change, Both Local and Global, https://doi.org/10.1007/s10712-019-09525-z, 2019.

Hersbach, H., Bell, B., Berrisford, P., Hirahara, S., Horányi, A., Muñoz-Sabater, J., Nicolas, J., Peubey, C., Radu, R., Schepers, D., Simmons, A., Soci, C., Abdalla, S., Abellan, X., Balsamo, G., Bechtold, P., Biavati, G., Bidlot, J., Bonavita, M., Chiara, G. D., Dahlgren, P., Dee, D., Diamantakis, M., Dragani, R., Flemming, J., Forbes, R., Fuentes, M., Geer, A., Haimberger, L., Healy, S., Hogan, R. J., Hólm, E., Janisková, M., Keeley, S., Laloyaux, P., Lopez, P., Lupu, C., Radnoti, G., de Rosnay, P., Rozum, I., Vamborg, F., Villaume, S., and Thépaut, J. N.: The ERA5 global reanalysis, Quarterly Journal of the Royal Meteorological Society, 146, https://doi.org/10.1002/qj.3803, 2020.

Hofer, S., Lang, C., Amory, C., Kittel, C., Delhasse, A., Tedstone, A., and Fettweis, X.: Greater Greenland Ice Sheet contribution to global sea level rise in CMIP6, Nature Communications, 11, https://doi.org/10.1038/s41467-020-20011-8, 2020.

Holube, K. M., Zolles, T., and Born, A.: Sources of uncertainty in Greenland surface mass balance in the 21st century, Cryosphere, 16, https://doi.org/10.5194/tc-16-315-2022, 2022.

Huybrechts, P. and Wolde, J. D.: The dynamic response of the Greenland and Antarctic ice sheets to multiple-century climatic warming, Journal of Climate, 12, https://doi.org/10.1175/1520-0442(1999)012<2169:tdrotg>2.0.co;2, 1999.

Knutti, R. and Sedláček, J.: Robustness and uncertainties in the new CMIP5 climate model projections, Nature Climate Change, 3, https://doi.org/10.1038/nclimate1716, 2013.

Larour, E., Seroussi, H., Morlighem, M., and Rignot, E.: Continental scale, high order, high spatial resolution, ice sheet modeling using the Ice Sheet System Model (ISSM), Journal of Geophysical Research: Earth Surface, 117, https://doi.org/10.1029/2011JF002140, 2012.

https://doi.org/10.5194/egusphere-2024-922
Preprint. Discussion started: 29 April 2024

Lee, V., Cornford, S. L., and Payne, A. J.: Initialization of an ice-sheet model for present-day Greenland, Annals of Glaciology, 56, https://doi.org/10.3189/2015AoG70A121, 2015.

Lipscomb, W. H., Price, S. F., Hoffman, M. J., Leguy, G. R., Bennett, A. R., Bradley, S. L., Evans, K. J., Fyke, J. G., Kennedy, J. H., Perego, M., Ranken, D. M., Sacks, W. J., Salinger, A. G., Vargo, L. J., and Worley, P. H.: Description and evaluation of the Community Ice Sheet Model (CISM) v2.1, Geoscientific Model Development, 12, https://doi.org/10.5194/gmd-12-387-2019, 2019.

Morlighem, M., Rignot, E., Seroussi, H., Larour, E., Dhia, H. B., and Aubry, D.: Spatial patterns of basal drag inferred using control methods from a full-Stokes and simpler models for Pine Island Glacier, West Antarctica, Geophysical Research Letters, 37, https://doi.org/10.1029/2010GL043853, 2010.

Morlighem, M., Williams, C. N., Rignot, E., An, L., Arndt, J. E., Bamber, J. L., Catania, G., Chauché, N., Dowdeswell, J. A., Dorschel, B., Fenty, I., Hogan, K., Howat, I., Hubbard, A., Jakobsson, M., Jordan, T. M., Kjeldsen, K. K., Millan, R., Mayer, L., Mouginot, J., Noël, B. P., O'Cofaigh, C., Palmer, S., Rysgaard, S., Seroussi, H., Siegert, M. J., Slabon, P., Straneo, F., van den Broeke, M. R., Weinrebe, W., Wood, M., and Zinglersen, K. B.: BedMachine v3: Complete Bed Topography and Ocean Bathymetry Mapping of Greenland From Multibeam Echo Sounding Combined With Mass Conservation, Geophysical Research Letters, 44, https://doi.org/10.1002/2017GL074954, 2017.

Pattyn, F., Perichon, L., Durand, G., Favier, L., Gagliardini, O., Hindmarsh, R. C., Zwinger, T., Albrecht, T., Cornford, S., Docquier, D., Fürst, J. J., Goldberg, D., Gudmundsson, G. H., Humbert, A., Hütten, M., Huybrechts, P., Jouvet, G., Kleiner, T., Larour, E., Martin, D., Morlighem, M., Payne, A. J., Pollard, D., Rückamp, M., Rybak, O., Seroussi, H., Thoma, M., and Wilkens, N.: Grounding-line migration in plan-view marine ice-sheet models: Results of the ice2sea MISMIP3d intercomparison, Journal of Glaciology, 59, https://doi.org/10.3189/2013JoG12J129, 2013.

Payne, A. J., Nowicki, S., Abe-Ouchi, A., Agosta, C., Alexander, P., Albrecht, T., Asay-Davis, X., Aschwanden, A., Barthel, A., Bracegirdle, T. J., Calov, R., Chambers, C., Choi, Y., Cullather, R., Cuzzone, J., Dumas, C., Edwards, T. L., Felikson, D., Fettweis, X., Galton-Fenzi, B. K., Goelzer, H., Gladstone, R., Golledge, N. R., Gregory, J. M., Greve, R., Hattermann, T., Hoffman, M. J., Humbert, A., Huybrechts, P., Jourdain, N. C., Kleiner, T., Munneke, P. K., Larour, E., clec'h, S. L., Lee, V., Leguy, G., Lipscomb, W. H., Little, C. M., Lowry, D. P., Morlighem, M., Nias, I., Pattyn, F., Pelle, T., Price, S. F., Quiquet, A., Reese, R., Rückamp, M., Schlegel, N. J., Seroussi, H., Shepherd, A., Simon, E., Slater, D., Smith, R. S., Straneo, F., Sun, S., Tarasov, L., Trusel, L. D., Breedam, J. V., van de Wal, R., van den Broeke, M., Winkelmann, R., Zhao, C., Zhang, T., and Zwinger, T.: Future Sea Level Change Under Coupled Model Intercomparison Project Phase 5 and Phase 6 Scenarios From the Greenland and Antarctic Ice Sheets, Geophysical Research Letters, 48, https://doi.org/10.1029/2020GL091741, 2021.

Pollard, D. and Deconto, R. M.: A simple inverse method for the distribution of basal sliding coefficients under ice sheets, applied to Antarctica, Cryosphere, 6, https://doi.org/10.5194/tc-6-953-2012, 2012.

Rignot, E., Box, J. E., Burgess, E., and Hanna, E.: Mass balance of the Greenland ice sheet from 1958 to 2007, Geophysical Research Letters, 35, https://doi.org/10.1029/2008GL035417, 2008.

Rückamp, M., Goelzer, H., and Humbert, A.: Sensitivity of Greenland ice sheet projections to spatial resolution in higher-order simulations: The Alfred Wegener Institute (AWI) contribution to ISMIP6 Greenland using the Ice-sheet and Sea-level System Model (ISSM), Cryosphere, 14, https://doi.org/10.5194/tc-14-3309-2020, 2020.

Seroussi, H., Morlighem, M., Rignot, E., Larour, E., Aubry, D., Dhia, H. B., and Kristensen, S. S.: Ice flux divergence anomalies on 79north Glacier, Greenland, Geophysical Research Letters, 38, https://doi.org/10.1029/2011GL047338, 2011.

Seroussi, H., Morlighem, M., Rignot, E., Khazendar, A., Larour, E., and Mouginot, J.: Dependence of century-scale projections of the Greenland ice sheet on its thermal regime, Journal of Glaciology, 59, https://doi.org/10.3189/2013JoG13J054, 2013.

https://doi.org/10.5194/egusphere-2024-922
Preprint. Discussion started: 29 April 2024

Seroussi, H., Morlighem, M., Larour, E., Rignot, E., and Khazendar, A.: Hydrostatic grounding line parameterization in ice sheet models, Cryosphere, 8, https://doi.org/10.5194/tc-8-2075-2014, 2014.

Shapiro, N. M. and Ritzwoller, M. H.: Inferring surface heat flux distributions guided by a global seismic model: Particular application to Antarctica, Earth and Planetary Science Letters, 223, https://doi.org/10.1016/j.epsl.2004.04.011, 2004.

Shepherd, A., Ivins, E. R., Geruo, A., Barletta, V. R., Bentley, M. J., Bettadpur, S., Briggs, K. H., Bromwich, D. H., Forsberg, R., Galin, N., Horwath, M., Jacobs, S., Joughin, I., King, M. A., Lenaerts, J. T., Li, J., Ligtenberg, S. R., Luckman, A., Luthcke, S. B., McMillan, M., Meister, R., Milne, G., Mouginot, J., Muir, A., Nicolas, J. P., Paden, J., Payne, A. J., Pritchard, H., Rignot, E., Rott, H., Sørensen, L. S., Scambos, T. A., Scheuchl, B., Schrama, E. J., Smith, B., Sundal, A. V., Angelen, J. H. V., Berg, W. J. V. D., Broeke, M. R. V. D., Vaughan, D. G., Velicogna, I., Wahr, J., Whitehouse, P. L., Wingham, D. J., Yi, D., Young, D., and Zwally, H. J.: A reconciled estimate of ice-sheet mass balance, Science, 338, https://doi.org/10.1126/science.1228102, 2012.

Shepherd, A., Ivins, E., Rignot, E., Smith, B., van den Broeke, M., Velicogna, I., Whitehouse, P., Briggs, K., Joughin, I., Krinner, G., Nowicki, S., Payne, T., Scambos, T., Schlegel, N., A, G., Agosta, C., Ahlstrøm, A., Babonis, G., Barletta, V. R., Bjørk, A. A., Blazquez, A., Bonin, J., Colgan, W., Csatho, B., Cullather, R., Engdahl, M. E., Felikson, D., Fettweis, X., Forsberg, R., Hogg, A. E., Gallee, H., Gardner, A., Gilbert, L., Gourmelen, N., Groh, A., Gunter, B., Hanna, E., Harig, C., Helm, V., Horvath, A., Horwath, M., Khan, S., Kjeldsen, K. K., Konrad, H., Langen, P. L., Lecavalier, B., Loomis, B., Luthcke, S., McMillan, M., Melini, D., Mernild, S., Mohajerani, Y., Moore, P., Mottram, R., Mouginot, J., Moyano, G., Muir, A., Nagler, T., Nield, G., Nilsson, J., Noël, B., Otosaka, I., Pattle, M. E., Peltier, W. R., Pie, N., Rietbroek, R., Rott, H., Sandberg Sørensen, L., Sasgen, I., Save, H., Scheuchl, B., Schrama, E., Schröder, L., Seo, K. W., Simonsen, S. B., Slater, T., Spada, G., Sutterley, T., Talpe, M., Tarasov, L., van de Berg, W. J., van der Wal, W., van Wessem, M., Vishwakarma, B. D., Wiese, D., Wilton, D., Wagner, T., Wouters, B., and Wuite, J.: Mass balance of the Greenland Ice Sheet from 1992 to 2018, Nature, 579, https://doi.org/10.1038/s41586-019-1855-2, 2020.

Slater, D. A., Straneo, F., Felikson, D., Little, C. M., Goelzer, H., Fettweis, X., and Holte, J.: Estimating Greenland tidewater glacier retreat driven by submarine melting, Cryosphere, 13, https://doi.org/10.5194/tc-13-2489-2019, 2019.

Slater, D. A., Felikson, D., Straneo, F., Goelzer, H., Little, C. M., Morlighem, M., Fettweis, X., and Nowicki, S.: Twenty-first century ocean forcing of the Greenland ice sheet for modelling of sea level contribution, https://doi.org/10.5194/tc-14-985-2020, 2020.

Sutterley, T. C., Velicogna, I., Csatho, B., Broeke, M. V. D., Rezvan-Behbahani, S., and Babonis, G.: Evaluating Greenland glacial isostatic adjustment corrections using GRACE, altimetry and surface mass balance data, Environmental Research Letters, 9, https://doi.org/10.1088/1748-9326/9/1/014004, 2014.

Vial, J., Dufresne, J. L., and Bony, S.: On the interpretation of inter-model spread in CMIP5 climate sensitivity estimates, Climate Dynamics, 41, https://doi.org/10.1007/s00382-013-1725-9, 2013.

Wake, L. M., Lecavalier, B. S., and Bevis, M.: Glacial Isostatic Adjustment (GIA) in Greenland: a Review, https://doi.org/10.1007/s40641-016-0040-z, 2016.

Yan, Q., Zhang, Z., Gao, Y., Wang, H., and Johannessen, O. M.: Sensitivity of the modeled present-day greenland ice Sheet to climatic forcing and spin-up methods and its influence on future sea level projections, Journal of Geophysical Research: Earth Surface, 118, https://doi.org/10.1002/jgrf.20156, 2013.

Yang, H., Krebs-Kanzow, U., Kleiner, T., Sidorenko, D., Rodehacke, C. B., Shi, X., Gierz, P., Niu, L., Gowan, E. J., Hinck, S., Liu, X., Stap, L. B., and Lohmann, G.: Impact of paleoclimate on present and future evolution of the Greenland Ice Sheet, PLoS ONE, 17, https://doi.org/10.1371/journal.pone.0259816, 2022.